ABOUT WAVELETS ON THE INTERVAL*

JEAN CHENG[1] AND WEI-CHANG SHANN[2]

Abstract. Wavelets on the closed interval are constructed step by step from the Daubechies' wavelets with compact supports. We follow mostly the guidelines by Andersson, Hall, Jawerth and Peters, with modifications on the construction of "edge" wavelets. Then we construct the filter operators discussed by Cohen, Daubechies and Vial. A filtering process is suggested for two-dimensional discrete transforms based on wavelets on the interval.

Key words. wavelets on the interval, filter

1. Introduction. Applying the general theory of multiresolution approximation for $L^2(\mathbb{R})$ by Mallat [8] and Meyer, Daubechies [5] constructed a family of wavelets with compact supports. We index this family of wavelets by a parameter p. The *mother* wavelet $\psi(x)$ has a support of length $2p-1$ and it is L^2-orthogonal to polynomials of degree $\leq p-1$. For wavelet theory and its applications in some branches of mathematics, we refer to Meyer [9].

The construction of various families of wavelets, their mathematical properties, their relations and applications to other disciplines are found in the "ten lectures" by Daubechies [6]. A concise overview of the compactly supported wavelets are found in the article by Strang [12]. Over there, the construction of this family of wavelets all start from a suitable sequence of *scaling coefficients* c_k, where $c_k \neq 0$ for $0 \leq k \leq 2p-1$ and $c_k = 0$ otherwise. These c_k shall satisfy certain conditions such that they are uniqely determined and there is a *scaling function* $\phi(x) \in L^2(\mathbb{R})$ such that

$$\phi(x) = \sum_k c_k \phi(2x-k) \tag{1.1}$$

with $\text{supp}\phi(x) = [0, 2p-1]$. This $\phi(x)$ generates a multiresolution approximation V_j of $L^2(\mathbb{R})$. Let $\phi_{jk}(x) = \sqrt{2^j}\phi(2^j x - k)$, then $\{\phi_{jk}(x) \mid k \in \mathbb{Z}\}$ is an orthonormal basis of V_j. The *mother* wavelet is then defined by

$$\psi(x) = \sum_k g_k \phi(2x-k).$$

Let $\psi_{jk}(x) = \sqrt{2^j}\psi(2^j x - k)$, then $\{\psi_{jk}(x) \mid (j,k) \in \mathbb{Z}^2\}$ is an orthonormal basis of $L^2(\mathbb{R})$. Here $g_k = (-1)^k c_{1-k}$, c_k and g_k is a pair of perfect reconstruction quadrature mirror filters.

A construction of wavelets on the interval was first proposed by Meyer [10]. However, there are a few shortcomings in this construction. Two groups (see next paragraph) of researchers were carrying out alternative constructions with better properties and more stable computational procedures. They lead to very similar constructions, thus a joint announcement by both groups was written in [3].

In Section 2, we following the guideline by Andersson, Hall, Jawerth and Peters [1] to construct the scaling functions $\phi_{jk}(x)$ and the multiresolution approximation on $L^2([0,1])$. In Section 3 we modify the approach in [1] to construct the wavelets $\psi_{jk}(x)$ on $L^2([0,1])$. This modification makes it more like the construction by Cohen, Daubechies and Vial [4]. In Section 4, again following [4], we describe the idea and construction of *prefilters*, then we propose a filtering process for two-dimensional discrete wavelet transforms based on wavelets on the interval.

---

* This work was supported by the National Science Coucil in Taiwan; grant #84-2121-M-008-009.

[1] E-mail address: zhenj@math.ncu.edu.tw.

[2] Department of Mathematics, National Central University, Chung-Li, Taiwan, R.O.C. E-mail address: shann@math.ncu.edu.tw

In the following, we sketch the construction step by step for the case of $p = 2$. At proper places we will indicate how would the parameters depend upon p. Note that all parameters can be computed from the scaling coefficients c_k and a few quadratures. Numerical methods are known for the computation of these quadratures in high precision [11].

2. Multiresolution on the interval. Let us assume the interval is $[0, 1]$. Near the left boundary $x = 0$, we define

$$\mathcal{X}_j^m(x) = \sqrt{2^j}(2^j x)^m;$$

near the right boundary $x = 1$,

$$\mathcal{Y}_j^m(x) = \mathcal{X}_j^m(x-1) = \sqrt{2^j}(2^j(x-1))^m.$$

Here m is an integer with $0 \le m \le (1 = p - 1)$.

We find the L^2-projection of $\mathcal{X}_j^m(x)$ in

$$V_j^L = \operatorname{span}\{\phi_{jk}(x) \mid k = (-2 = 2 - 2p), -1, \ldots, (0 = \delta_L - 1)\};$$

and $\mathcal{Y}_j^m(x)$ in

$$V_j^R = \operatorname{span}\{\phi_{jk}(x) \mid k = (2^j - 3 = 2^j - 2p + 2 - \delta_R), 2^j - 2, \ldots, 2^j - 1\}.$$

Here δ_L and δ_R are the parameters defined in [1] which indicate the number of "interior" basis functions that are included for the orthonormalization process near the boundary points. Following [4], we see that it makes more sense for $\delta_L \ge 1$ and $\delta_R \ge 1$. In this article we assume that $\delta_L = \delta_R = 1$ (same as in [4]). See remarks by the end of this section. We further assume that

$$j \ge 3 = \lceil \log_2 2p - 1 \rceil + 1;$$

that is, $V_j^L \cap V_j^R = \emptyset$.

Let x_k^m be the component of $\mathcal{X}_j^m$ in $\phi_{jk}(x)$:

$$x_k^m = (\mathcal{X}_j^m, \phi_{jk}) = \int (x + k)^m \phi(x)\, dx = \sum_{i=0}^{m} \binom{m}{i} k^i M_{m-i}$$

Here $M_i = \int x^i \phi(x)\, dx$, it is well known that these quadratures can be obtained as accurate as the scaling coefficients c_k. We see that x_k^m are independent of j. The components y_k^m are similarly defined and are independent of j.

Now we have the projected functions on $[0, 1]$:

$$X_j^m = \sum_{k=-2}^{0} x_k^m \phi_{jk}|_{[0,1]}, \quad Y_j^m = \sum_{k=2^j-3}^{2^j-1} y_k^m \phi_{jk}|_{[0,1]}.$$

Obviously $\{X_j^m\}_{m=0}^1$ and $\{Y_j^m\}_{m=0}^1$ are linearly independent, and they are orthogonal with the "interior" scaling functions $\{\phi_{jk}\}_{k=1}^{2^j-4}$, which are already orthonormal. See Figure 1, note that they are actually polynomials near the boundary points. So, we would only have to orthonormalize X_j^m

and Y_j^m near the boundary points. The result will be an orthonormal set. Let $V_j[0,1]$ be the linear space spanned by this orthonormal set. Then

$$\dim V_j[0,1] = 2^j, \quad j \geq 3.$$

The orthonormalization process is done by taking the squared root inverse of the mass matrices of $\{X_j^m\}$ and $\{Y_j^m\}$. Let $\mathbf{X} = (X_{mn})$ where

$$X_{mn} = (X_j^m, X_j^n).$$

$\mathbf{X}$ is symmetric and positive definite, and it is actually independent of j:

$$\begin{aligned}
X_{00} &= 1 + N_1 + 2N_2 + N_3, \\
X_{01} &= x_{-2}^1(N_1 + N_2) + x_{-1}^1(N_2 + N_3) + x_0^1, \\
X_{11} &= (x_{-2}^1)^2 N_1 + (x_{-1}^1)^2 N_3 + (x_0^1)^2 + 2x_{-2}^1 x_{-1}^1 N_2
\end{aligned}$$

The accuracy of $\mathbf{X}$ is totally determined by the numerical quadratures

$$\begin{aligned}
N_1 &= \int_0^\infty \phi(x+2)\phi(x+2)\,dx, \\
N_2 &= \int_0^\infty \phi(x+2)\phi(x+1)\,dx, \\
N_3 &= \int_0^\infty \phi(x+1)\phi(x+1)\,dx.
\end{aligned}$$

Numerical methods that compute N_* in high precision are described in [11].

The mass matrix $\mathbf{Y}$ is similarly defined for $\{Y_j^m\}$, and the entries are

$$\begin{aligned}
Y_{00} &= 3 - N_1 - 2N_2 - N_3, \\
Y_{01} &= y_{jr_1}^1 + y_{jr_2}^1(1 - N_1 - N_2) + y_{jr_3}^1(1 - N_2 - N_3), \\
Y_{11} &= (y_{jr_1}^1)^2 + (y_{jr_2}^1)^2(1 - N_1) + (y_{jr_3}^1)^2(1 - N_3) - 2y_{jr_2}^1 y_{jr_3}^1 N_2.
\end{aligned}$$

Here, for convenience, we define $r_0 = 2^j - 4$, which is the last "interior" basis function at level j, and $r_i = r_0 + i$, for $i = 1, 2, 3$. The value j will be clear in the context.

There exist $\mathbf{S} = \mathbf{X}^{-1/2}$ and $\mathbf{T} = \mathbf{Y}^{-1/2}$. Let

$$\begin{pmatrix} \varphi_{j,-1}(x) \\ \varphi_{j,0}(x) \end{pmatrix} = \mathbf{S} \begin{pmatrix} X_j^0(x) \\ X_j^1(x) \end{pmatrix}, \quad \begin{pmatrix} \varphi_{jr_1}(x) \\ \varphi_{jr_2}(x) \end{pmatrix} = \mathbf{T} \begin{pmatrix} Y_j^0(x) \\ Y_j^1(x) \end{pmatrix}.$$

In the following we will denote the original compactly supported scaling functions by ϕ and the new scaling functions on $[0,1]$ by φ. One should understand that $\varphi_{jk} = \phi_{jk}$ for $1 \leq k \leq r_0$. Then

$$\{\varphi_{j,-1}, \varphi_{j0}, \varphi_{j1}, \ldots, \varphi_{jr_0}, \varphi_{jr_1}, \varphi_{jr_2}\}$$

is an orthonormal basis of $V_j[0,1]$. See Figure 2.

Theoretically $V_j[0,1]$ preserve the nested relation [3]:

$$V_j[0,1] \subset V_{j+1}[0,1]$$

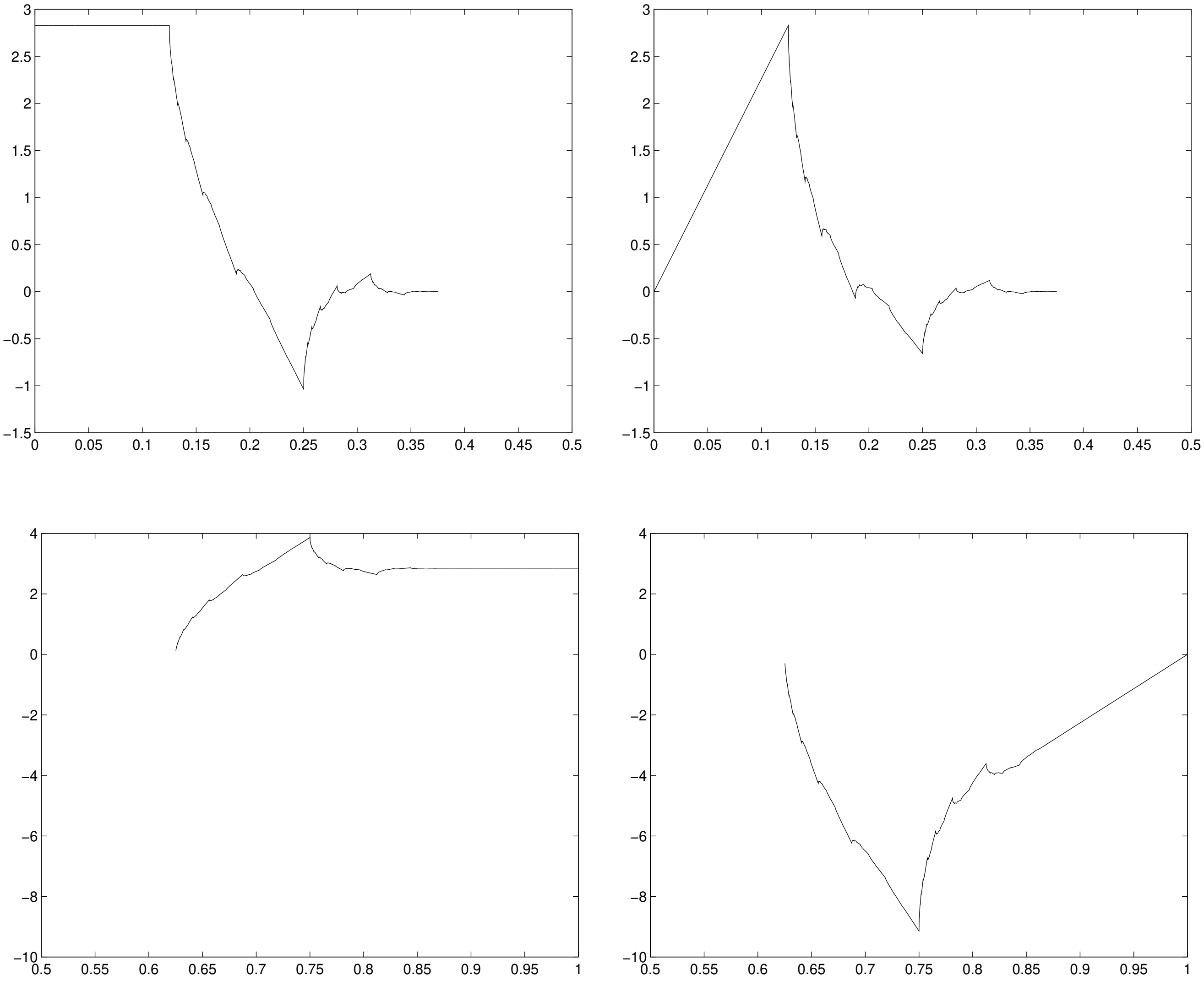

Figure 1. The nonzero part of $X_3^0(x)$ (top left), $X_3^1(x)$ (top right), $Y_3^0(x)$ (bottom left) and $Y_3^1(x)$.

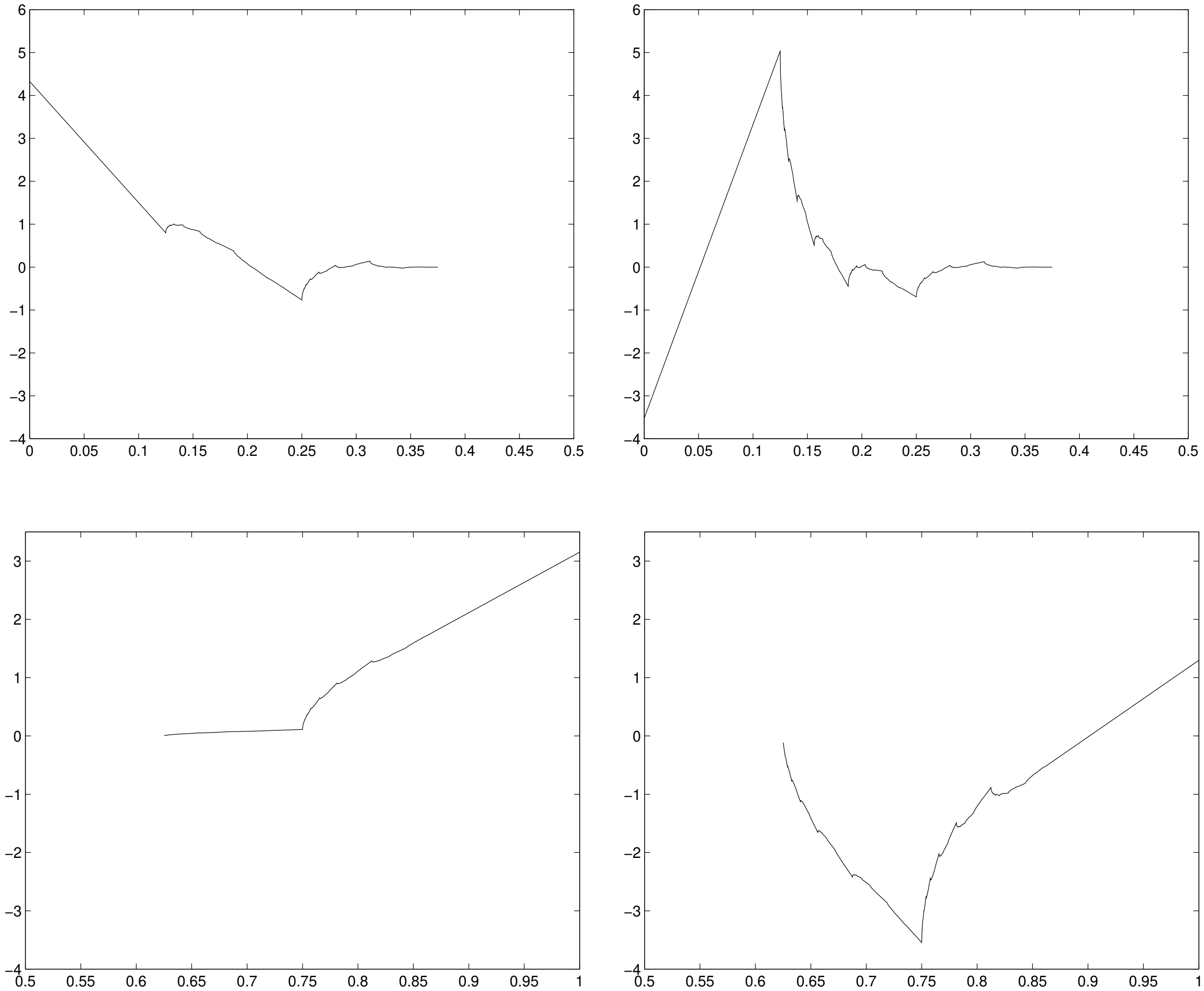

Figure 2. The nonzero part of $\phi_{3,-1}(x)$ (top left), $\phi_{30}(x)$ (top right), $\phi_{3r_1}(x)$ (bottom left) and $\phi_{3r_2}(x)$.

However, there will be different sets of scaling equations for the "left," "interior" and "right" basis functions. Those for the "interior" scaling functions are identically inherit from the original scaling equation (1.1). Those for the two edges will be numerically determined as following.

We now build the low pass filter, H. Let us illustrate the idea by the projection from $V_4[0,1]$ onto $V_3[0,1]$. Let

$$\Phi_3 = \begin{pmatrix} \phi_{3,-1} \\ \phi_{3,0} \\ \phi_{3,1} \\ \vdots \\ \phi_{3,4} \\ \phi_{3,5} \\ \phi_{3,6} \end{pmatrix}, \quad \Phi_4 = \begin{pmatrix} \phi_{4,-1} \\ \phi_{4,0} \\ \phi_{4,1} \\ \vdots \\ \phi_{4,12} \\ \phi_{4,13} \\ \phi_{4,14} \end{pmatrix}.$$

We will determine H such that

$$\Phi_3 = H\Phi_4.$$

Now $H = (H_{mn})$ is an 8×16 matrix determined by

$$H_{mn} = (\phi_{3m}, \phi_{4n}).$$

We partition H into 9 parts according to the index m, n being in the "left," "interior" or "right" portion of the basis functions.

$$H = \begin{pmatrix} H_{LL} & H_{LI} & H_{LR} \\ H_{IL} & H_{II} & H_{IR} \\ H_{RL} & H_{RI} & H_{RR} \end{pmatrix}$$

We find H_{LL} is a 2×2 matrix with

$$\begin{aligned} H_{LL} &= \begin{pmatrix} (\phi_{3,-1}, \phi_{4,-1}) & (\phi_{3,-1}, \phi_{4,0}) \\ (\phi_{3,0}, \phi_{4,-1}) & (\phi_{3,0}, \phi_{4,0}) \end{pmatrix} \\ &= \mathbf{S} \begin{pmatrix} (X_3^0, X_4^0) & (X_3^0, X_4^1) \\ (X_3^1, X_4^0) & (X_3^1, X_4^1) \end{pmatrix} \mathbf{S}^t. \end{aligned}$$

H_{LI} is a 2×12 matrix which are zeros except for the first 3 columns:

$$\begin{aligned} &\begin{pmatrix} (\phi_{3,-1}, \phi_{4,1}) & (\phi_{3,-1}, \phi_{4,2}) & (\phi_{3,-1}, \phi_{4,3}) \\ (\phi_{3,0}, \phi_{4,1}) & (\phi_{3,0}, \phi_{4,2}) & (\phi_{3,0}, \phi_{4,3}) \end{pmatrix} \\ =&\frac{1}{\sqrt{2}} \mathbf{S} \begin{pmatrix} c_1 + c_3 & c_2 & c_3 \\ x_{-1}^1 c_1 + x_0^1 c_3 & x_0^1 c_2 & x_0^1 c_3 \end{pmatrix} \end{aligned}$$

H_{II} is a familiar matrix of dimension 4×12.

$$\begin{aligned} H_{II} &= \begin{pmatrix} (\phi_{3,1}, \phi_{4,1}) & (\phi_{3,1}, \phi_{4,2}) & \ldots & (\phi_{3,1}, \phi_{4,12}) \\ (\phi_{3,2}, \phi_{4,1}) & (\phi_{3,2}, \phi_{4,2}) & \ldots & (\phi_{3,2}, \phi_{4,12}) \\ (\phi_{3,3}, \phi_{4,1}) & (\phi_{3,3}, \phi_{4,2}) & \ldots & (\phi_{3,3}, \phi_{4,12}) \\ (\phi_{3,4}, \phi_{4,1}) & (\phi_{3,4}, \phi_{4,2}) & \ldots & (\phi_{3,4}, \phi_{4,12}) \end{pmatrix} \\ &= \frac{1}{\sqrt{2}} \begin{pmatrix} 0 & c_0 & c_1 & c_2 & c_3 & 0 & 0 & 0 & 0 & 0 & 0 & 0 \\ 0 & 0 & 0 & c_0 & c_1 & c_2 & c_3 & 0 & 0 & 0 & 0 & 0 \\ 0 & 0 & 0 & 0 & 0 & c_0 & c_1 & c_2 & c_3 & 0 & 0 & 0 \\ 0 & 0 & 0 & 0 & 0 & 0 & 0 & c_0 & c_1 & c_2 & c_3 & 0 \end{pmatrix} \end{aligned}$$

Similar to H_{LI}, H_{RI} are zeros except for the last three columns:

$$\begin{pmatrix} (\phi_{3,5},\phi_{4,10}) & (\phi_{3,5},\phi_{4,11}) & (\phi_{3,5},\phi_{4,12}) \\ (\phi_{3,6},\phi_{4,10}) & (\phi_{3,6},\phi_{4,11}) & (\phi_{3,6},\phi_{4,12}) \end{pmatrix}$$
$$= \frac{1}{\sqrt{2}} \mathbf{T} \begin{pmatrix} c_0 & c_1 & c_2 + c_0 \\ y_5^1 c_0 & y_5^1 c_1 & y_5^1 c_2 + y_6^1 c_0 \end{pmatrix}$$

And H_{RR} is a 2×2 matrix with

$$\begin{aligned} H_{RR} &= \begin{pmatrix} (\phi_{3,5},\phi_{4,13}) & (\phi_{3,5},\phi_{4,14}) \\ (\phi_{3,6},\phi_{4,13}) & (\phi_{3,6},\phi_{4,14}) \end{pmatrix} \\ &= \mathbf{T} \begin{pmatrix} (Y_3^0, Y_4^0) & (Y_3^0, Y_4^1) \\ (Y_3^1, Y_4^0) & (Y_3^1, Y_4^1) \end{pmatrix} \mathbf{T}^t \end{aligned}.$$

By orthogonality, $H_{LR}, H_{IL}, H_{IR}, H_{RL}$ are zero matrices.

In general, note that the dimension of H depends on the level index j; that is, $2^j \times 2^{j+1}$. However, the nonzero entries in the "boarder" parts of H do not depend on j, only the "interior" part H_{II} does. H_{LL} and H_{RR} are $p \times p$ matrices, and the nonzero parts of H_{LI} and H_{RI} are $p \times (2p-1)$. The "interior" part inherits the pyramid algorithm for the original compactly supported low pass filters [7].

Note that $V_j[0,1] \neq V_j|_{[0,1]}$. However,

$$V_3[0,1] \subset V_4[0,1] \subset \cdots$$

and $\cup V_j[0,1]$ is dense in $L^2([0,1])$. The choice of $\delta_L = \delta_R = 1$ makes $\dim V_j[0,1] = 2^j$. Hence there will be an equal dimension for $V_j[0,1]$ and $W_j[0,1]$. Functions in $V_j[0,1]$ are actually polynomials in the intervals $[0, \delta_L/2^j]$ and $[1-\delta_R/2^j, 1]$, so they are smooth (Figure 2).

3. Wavelets on the interval. As in the framework of multiresolution approximation of $L^2(\mathbb{R})$, we now decompose

$$V_{j+1}[0,1] = V_j[0,1] \oplus W_j[0,1].$$

That is, define $W_j[0,1]$ to be the subspace of $V_{j+1}[0,1]$ which is orthogonal to $V_j[0,1]$. Clearly we have

$$\dim W_j[0,1] = 2^j.$$

The wavelets on interval are the orthonormal basis functions for $W_j[0,1]$.

The original compactly supported wavelets satisfy

$$\psi_{j,k} = \frac{1}{\sqrt{2}} \sum_l g_{l-2k} \phi_{j+1,l}.$$

Since $g_{l-2k} \neq 0$ only for $(-2 = 2-2p) \leq l - 2k \leq 1$, thus

$$\begin{aligned} &\begin{cases} 1 \leq l \leq 2^{j+1} - 4 \\ -2 > -2k \\ 1 < 2^{j+1} - 4 - 2k \end{cases} \\ \Rightarrow \quad & 2 \leq k \leq (2^j - 3 = 2^j - p - 1) \\ \Rightarrow \quad & \psi_{jk}(x) \in V_{j+1}[0,1], \quad \text{for } 2 \leq k \leq 2^j - 3. \end{aligned}$$

But we would like to shift our *mother* wavelet such that $\text{supp}\psi(x) = [0, 2p-1]$, thus the index would be shifted such that

$$\psi_{jk}(x) \in V_{j+1}[0,1], \quad \text{for } 1 \leq k \leq 2^j - 4 = r_0.$$

That is, we already have $2^j - 4$ orthonormal basis on $W_j[0,1]$, which are the original compactly supported wavelets. We need $4 = 2p$ more basis functions for $W_j[0,1]$; they are selected such that there are $2 = p$ basis functions near each boundary point.

From above, we know the orthonormal bases for $V_j[0,1]$ and $V_{j+1}[0,1]$, and we have $2^j - 4$ basis functions on $W_j[0,1]$. Now we want the basis functions of $V_{j+1}[0,1]$ which do not belong to the span of $V_j[0,1]$ and $\{\psi_{j,k}\}_{k=1}^{r_0}$. Then we find their components which are orthogonal to $V_j[0,1]$. The result will be functions in $W_j[0,1]$.

We can show that

$$\begin{aligned} \phi(x)_{j+1,-1} &\notin \text{span}\{V_j[0,1] \cup \{\psi_{jk}\}_{k=1}^{r_0}\}, \\ \phi(x)_{j+1,0} &\notin \text{span}\{V_j[0,1] \cup \{\psi_{jk}\}_{k=1}^{r_0} \cup \phi(x)_{j+1,-1}\}. \end{aligned}$$

Hence, on the "left," we choose the orthogonal complements of $\phi_{j+1,-1}$ and $\phi_{j+1,0}$; similarly, on the "right," we choose ϕ_{j+1,r_1} and ϕ_{j+1,r_2}. Define the complement functions:

$$\begin{aligned} \phi_{j0}^L &= \phi_{j+1,-1} - P_j\phi_{j+1,-1} \\ \phi_{j1}^L &= \phi_{j+1,0} - P_j\phi_{j+1,0} \\ \phi_{j0}^R &= \phi_{j+1,r_1} - P_j\phi_{j+1,r_1} \\ \phi_{j1}^R &= \phi_{j+1,r_2} - P_j\phi_{j+1,r_2} \end{aligned}$$

Here P_j is the L^2-orthogonal projection from $L^2([0,1])$ onto $V_j[0,1]$. Then $\phi_{j*}^* \in W_j[0,1]$ and it can be shown that they are linearly independent. They are already orthogonal with the "interior" wavelets $\{\psi_{jk}\}_{k=1}^{r_0}$. Now we orthonormalize ϕ_{j*}^* to get a set of orthonormal basis for $W_j[0,1]$.

As for the orthonormalization for scaling functions on the "edge," we need the mass matrix of ϕ_{j*}^L, say $\mathbf{X}^\perp$, and that of ϕ_{j*}^R, say $\mathbf{Y}^\perp$. It turns out that we do not need much more calculations,

$$\mathbf{X}^\perp = I - H_{LL}^t H_{LL}, \quad \mathbf{Y}^\perp = I - H_{RR}^t H_{RR}.$$

Here I is the identity matrix of compatible dimension, eg, 2×2 for this case. Again, $\mathbf{X}^\perp$ and $\mathbf{Y}^\perp$ are symmetric positive definite and they are independent of j. Now define

$$\begin{pmatrix} \psi_{j,-1}(x) \\ \psi_{j,0}(x) \end{pmatrix} = (\mathbf{X}^\perp)^{-\frac{1}{2}} \begin{pmatrix} \phi_{j0}^L(x) \\ \phi_{j1}^L(x) \end{pmatrix}, \quad \begin{pmatrix} \psi_{j,r_1}(x) \\ \psi_{j,r_2}(x) \end{pmatrix} = (\mathbf{Y}^\perp)^{-\frac{1}{2}} \begin{pmatrix} \phi_{j0}^R(x) \\ \phi_{j1}^R(x) \end{pmatrix}.$$

In the following we will denote the original compactly supported wavelets by ψ and the new wavelets on $[0,1]$ by ψ. One should understand that $\psi_{jk} = \psi_{jk}$ for $1 \leq k \leq r_0$. Then

$$\{\psi_{j,-1}, \psi_{j0}, \psi_{j1}, \ldots, \psi_{jr_0}, \psi_{jr_1}, \psi_{jr_2}\}$$

forms an orthonormal basis of $W_j[0,1]$. See Figure 3.

For the relation between $V_{j+1}[0,1]$ and $W_j[0,1]$, it amounts to construct the high pass filter, G. Again, we illustrate the idea by the projection from $V_4[0,1]$ onto $W_3[0,1]$. Let

$$\Psi_3 = \begin{pmatrix} \psi_{3,-1} \\ \psi_{3,0} \\ \psi_{3,1} \\ \vdots \\ \psi_{3,4} \\ \psi_{3,5} \\ \psi_{3,6} \end{pmatrix}, \quad \Phi_4 = \begin{pmatrix} \phi_{4,-1} \\ \phi_{4,0} \\ \phi_{4,1} \\ \vdots \\ \phi_{4,12} \\ \phi_{4,13} \\ \phi_{4,14} \end{pmatrix}$$

We will determine G such that

$$\Psi_3 = G\Phi_4.$$

Now G is a $(8 = 2^j) \times (16 = 2^{j+1})$ matrix. We partition G in the same pattern as for H,

$$G = \begin{pmatrix} G_{LL} & G_{LI} & G_{LR} \\ G_{IL} & G_{II} & G_{IR} \\ G_{RL} & G_{RI} & G_{RR} \end{pmatrix}.$$

After some manipulations, we can write G in terms of H:

$$\begin{aligned} G_{LL} &= (I - H_{LL}^t H_{LL})^{\frac{1}{2}} \\ G_{LI} &= -(I - H_{LL}^t H_{LL})(H_{LL}^t H_{LI}) \\ G_{RI} &= -(I - H_{RR}^t H_{RR})(H_{RR}^t H_{RI}) \\ G_{RR} &= (I - H_{RR}^t H_{RR})^{\frac{1}{2}} \end{aligned}$$

The remarks for H also apply to G. Hence all but a fixed small number $(2p)$ of filter coefficients are the same as the original compactly supported wavelets. From the construction, we have

$$H^t H + G^t G = I.$$

Therefore, the fast pyramid decomposition and reconstruction algorithm of Mallat [7] is almost totally preserved.

4. Pre-filters. In the application of discrete wavelet transforms, the signals (or images) are in discrete values; namely in form of vectors or matrices. In this case, as pointed out in [4], the discrete wavelets transform on the interval has a shortcoming. The decomposed data may have larger high frequency components than the periodized discrete wavelet transform, as illustrated in Figures 4.

Let us explain the situation for the case of $p = 2$. For wavelets of this approximation order, polynomials of degree 0 and 1 are in V_j, in the following rough sense:

$$1 = \sum_k (1,\ \phi_{jk})\phi_{jk} \quad x = \sum_k (x,\ \phi_{jk})\phi_{jk}$$

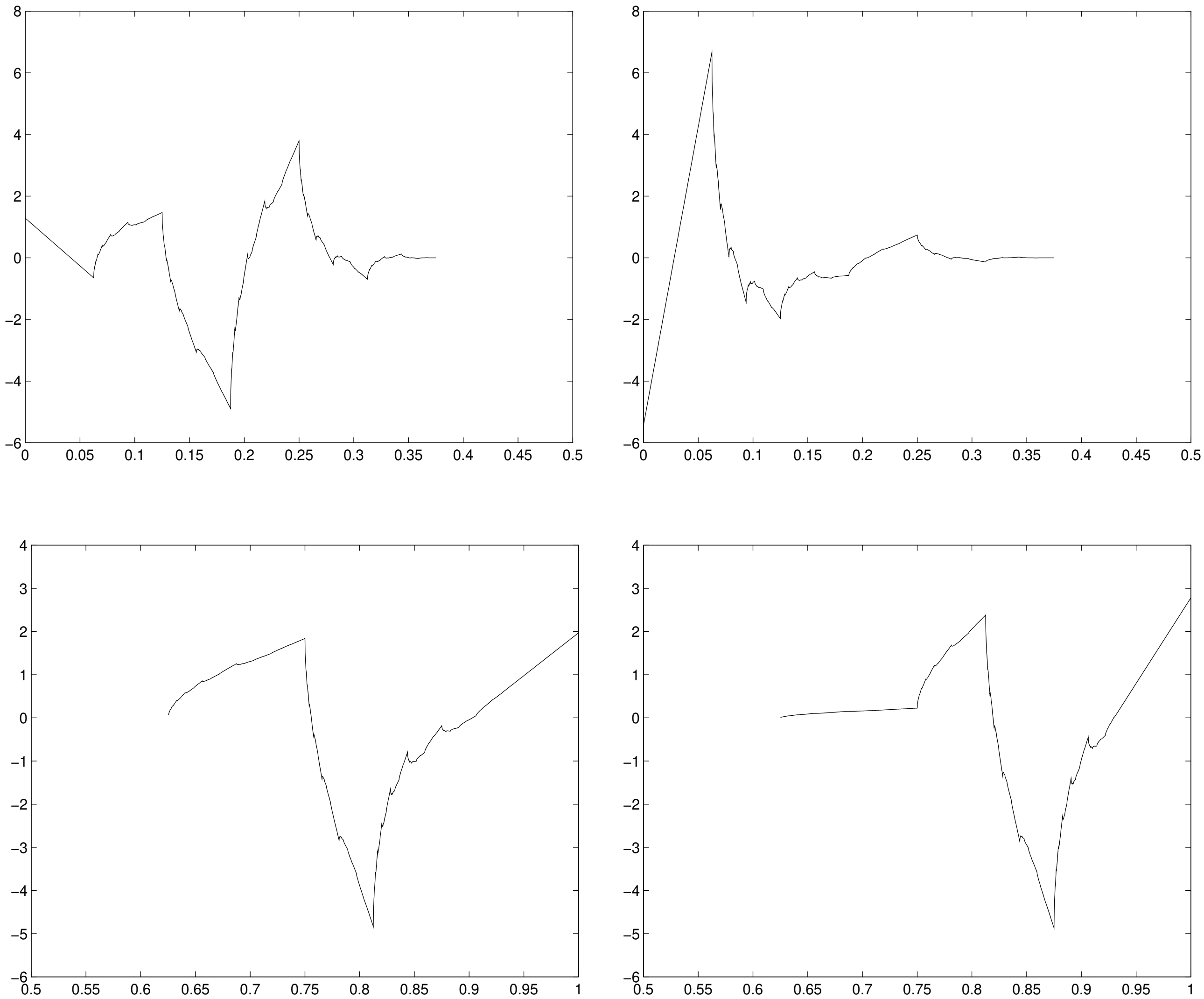

Figure 3. The nonzero part of $\psi_{3,-1}(x)$ (top left), $\psi_{30}(x)$ (top right), $\psi_{3r_1}(x)$ (bottom left) and $\psi_{3r_2}(x)$.

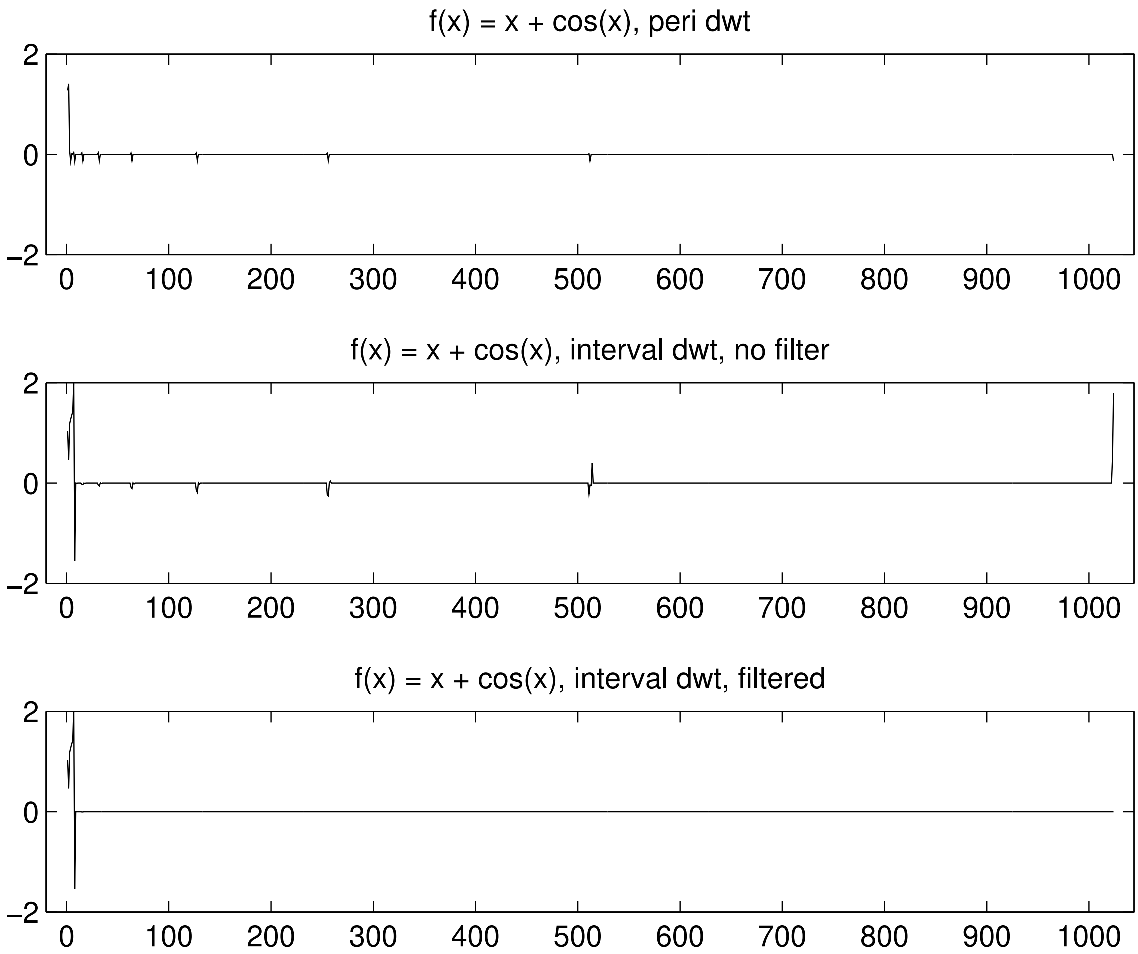

Figure 4. If we take 1024 samples from $f(x) = x + \cos x$ in $[0, 1]$ and perform the periodized discrete wavelet transform (DWT), that is, extend $f(x)$ periodically on $\mathbb{R}$ and perform the DWT. There are artificial high amplitudes in each W_j due to the discontinuity introduced by the periodic extension (top). When the interval DWT is applied without the filtering process, the amplitudes are even larger (middle). However, the interval DWT with filtering process results flat high frequency signals. It is because $\cos x$ is smooth and the (processed) high pass filter annihilates x.

For wavelets on the interval, it is true that we still have:

$$1 = \sum_{k=-1}^{2^j-2} (1,\ \phi_{jk})\phi_{jk} \quad x = \sum_{k=-1}^{2^j-2} (x,\ \phi_{jk})\phi_{jk}$$

However, $(1, \phi_{jk}) = 1$ and $(x, \phi_{jk}) = k + M_1$. Hence the vectors corresponding to the projection coefficients of 1 and x in V_0 are essentially

$$\mathbf{x}_0 = (\ldots, 1, 1, 1, \ldots)^t \text{ and } \mathbf{x}_1 = (\ldots, 1, 2, 3, \ldots)^t. \tag{4.1}$$

While these two vectors can be annihilated by the high pass filter of the discrete wavelet transform (DWT), it is no longer true for our new DWT based on wavelets on the interval. In practice, signals are pointwise values of a function whose most significant parts are in the polynomials of low degree; that is, in the form of

$$\alpha_0\mathbf{x}_0 + \alpha_1\mathbf{x}_1 + \cdots,$$

where α_0 and α_1 are relatively large. The periodized high pass filter annihilates entire $\mathbf{x}_0$ and most part of $\mathbf{x}_1$, while the interval high pass filter fails to do that. Sometimes, as we see in Figure 4, it may introduce very large high frequency components (very large coefficients in $W_j[0,1]$ for high j).

However, the projection coefficients of 1 and x onto $V_j[0,1]$ are still in the form of (4.1), except for the first and last two (p) components. The idea of the *prefilter* in [4] is to transform the space $\text{span}\{\mathbf{x}_0, \mathbf{x}_1\}$ into which can be annihilated by the high pass filter G. That is, essentially

$$\begin{pmatrix} 1 \\ 1 \\ 1 \\ \vdots \\ 1 \\ 1 \\ 1 \end{pmatrix} + \begin{pmatrix} 1 \\ 2 \\ 3 \\ \vdots \\ 2^j-2 \\ 2^j-1 \\ 2^j \end{pmatrix} \mapsto \begin{pmatrix} \int \phi_{j,-1} \\ \int \phi_{j0} \\ \int \phi_{j1} \\ \vdots \\ \int \phi_{j,r_0} \\ \int \phi_{j,r_1} \\ \int \phi_{j,r_2} \end{pmatrix} + \begin{pmatrix} \int x\phi_{j,-1} \\ \int x\phi_{j0} \\ \int x\phi_{j1} \\ \vdots \\ \int x\phi_{j,r_0} \\ \int x\phi_{j,r_1} \\ \int x\phi_{j,r_2} \end{pmatrix}$$

Since the spaces are different only at the first and last two entries, this amounts to find linear operators F_L and F_R such that

$$F_L : \text{span}\{\begin{pmatrix} \int \phi_{j,-1} \\ \int \phi_{j,0} \end{pmatrix}, \begin{pmatrix} \int x\phi_{j,-1} \\ \int x\phi_{j,0} \end{pmatrix}\} \mapsto \text{span}\{\begin{pmatrix} \int \phi_{j,-1} \\ \int \phi_{j,0} \end{pmatrix}, \begin{pmatrix} \int x\phi_{j,-1} \\ \int x\phi_{j,0} \end{pmatrix}\}$$

$$F_R : \text{span}\{\begin{pmatrix} \int \phi_{j,2^j-3} \\ \int \phi_{j,2^j-2} \end{pmatrix}, \begin{pmatrix} \int x\phi_{j,2^j-3} \\ \int x\phi_{j,2^j-2} \end{pmatrix}\} \mapsto \text{span}\{\begin{pmatrix} \int \phi_{j,2^j-3} \\ \int \phi_{j,2^j-2} \end{pmatrix}, \begin{pmatrix} \int x\phi_{j,2^j-3} \\ \int x\phi_{j,2^j-2} \end{pmatrix}\}$$

Since the vectors listed above are linearly independent, so F_L and F_R will be non-singular matrices. After some linear combinations of the basis functions in these subspaces, we observe that F_L and F_R are actually independent of j:

$$F_L = \mathbf{S}\tilde{\mathbf{X}} \begin{pmatrix} K_2^0 & -M_1K_2^0 + K_2^1 \\ K_1^0 & -M_1K_1^0 + K_1^1 \\ 1 & 0 \end{pmatrix} \begin{pmatrix} 1 & -1 \\ 1 & 0 \end{pmatrix}^{-1}$$

$$F_R = \mathbf{T}\tilde{\mathbf{Y}} \begin{pmatrix} 1 & -1 \\ 1 - K_2^0 & K_2^0(M_1-2) - K_2^1 \\ 1 - K_1^0 & K_1^0(M_1-2) - K_1^1 + 1 \end{pmatrix} \begin{pmatrix} 1 & -1 \\ 1 & 0 \end{pmatrix}^{-1}$$

where

$$\tilde{\mathbf{X}} = \begin{pmatrix} x^0_{-2} & x^0_{-1} & x^0_0 \\ x^1_{-2} & x^1_{-1} & x^1_0 \end{pmatrix}, \quad \tilde{\mathbf{Y}} = \begin{pmatrix} y^0_{2^j-2} & y^0_{2^j-2} & y^0_{2^j-2} \\ y^1_{2^j-2} & y^1_{2^j-1} & y^1_{2^j-1} \end{pmatrix}.$$

Here $K^m_n = \int_0^\infty x^m \phi(x+n)\,dx$. Note that $m \geq 0$ and $1 \leq n \leq (2 = 2p-2)$ are the meaningful indices. We also follow [11] for high accurate values of K^m_n.

Now we have the 2×2 (or $p \times p$) filter matrices F_L and F_R. For one-dimensional data (signals), we preprocess the input $v = (v_0, v_1, \ldots, v_n)^t$ by converting it to $\tilde{v} = (\tilde{v}_0, \tilde{v}_1, v_2, \ldots, v_{n-2}, \tilde{v}_{n-1}, \tilde{v}_n)^t$, where

$$\begin{pmatrix} \tilde{v}_0 \\ \tilde{v}_1 \end{pmatrix} = F_L \begin{pmatrix} v_0 \\ v_1 \end{pmatrix}, \quad \begin{pmatrix} \tilde{v}_{n-1} \\ \tilde{v}_n \end{pmatrix} = F_R \begin{pmatrix} v_{n-1} \\ v_n \end{pmatrix}.$$

Then we perform the interval DWT on $\tilde{v}$. Reversely, we post-process $\tilde{v}$ by F_L^{-1} and F_R^{-1} after the inverse transform. See also Figure 4 for a demonstration. There is almost no operation count added by the pre- and post-process.

For two-dimensional data (images), however, we need the preprocess on the two "boarder" rows and columns. Assume that one level of the two-dimensional wavelet transform is implemented by applying one level of the one-dimensional wavelet transform on each row of data, followed by one level of the one-dimensional wavelet transform on each column of data. See [7]. In this case, multiplying F_L (F_R) to the first (last) two rows and columns will not work for our purpose.

The key point of the filtering process is to keep the polynomials 1, x, y and xy invariant under the low pass filter, while orthogonal to the high pass filter. Keep this in mind, we find a successful filtering process. That is, we apply the prefilters to column vectors, perform interval DWT on each row, undo the prefilters (switch it back to the original space), then apply the prefilters to row vectors and perform the interval DWT on each column, then undo the prefilters. The inverse transform needs reversed processes. For coding details, we refer to the master dissertation of the first author, Miss Cheng [2]. Figure 5 shows the effect of this filtering process.

Our filtering process introduces $O(pN)$ of operation count to the computational complexity, where N is the dimension of input matrix. Whether it worths the efforts is yet to be seen by more experiments on actual image samples. More can be found in [2].

REFERENCES

[1] L. Andersson, N. Hall, B. Jawerth and G. Peters, *Wavelets on closed subsets of the real line,* in "Recent advances in wavelet analysis," Academic Press, Boston, 1994, pp. 1–61.

[2] J. Cheng, *The construction of wavelets on the interval and a prefilter process for wavelet transforms,* Master Dissertation, Department of Mathematics, National Central University, 1995.

[3] A. Cohen, I. Daubechies, B. Jawerth and P. Vial, *Multiresolution analysis, wavelets and fast algorithms on the interval,* C. R. Acad. Sci. Paris, Série I, 316 (1992), pp. 417–421.

[4] A. Cohen, I. Daubechies and P. Vial, *Wavelets on the interval and fast wavelet transforms,* Appl. Comput. Harmonic Anal., 1 (1993), pp. 54–81.

[5] I. Daubechies, *Orthonormal bases of compactly supported wavelets,* Comm. Pure Appl. Math., 41 (1988), pp. 909–996.

[6] I. Daubechies, "Ten lectures on wavelets," SIAM, Philadelphia, 1992.

[7] S. Mallat, *Multiresolution approximations and wavelet orthonormal bases of $L^2(\mathbb{R})$,* Trans. Amer. Math. Soc., 315 (1989), pp. 69–87.

[8] S. Mallat, *A theory for multiresolution signal decomposition: The wavelet representation,* IEEE Trans. on Patt. Anal. Mach. Intell., 11 (1989), pp. 674–693.

[9] Y. Meyer, “Ondelletes et fonctions splines,” Seminaire Equations aux Derivees Partielles, Ecole Polytechnique, Paris, 1986.

[10] Y. Meyer, *Ondelettes sur l'intervalle,* Rev. Math. Iberoamer., 7 (1992), pp. 115–133.

[11] W.-C. Shann and C.-C. Yen, *Quadratures involving polynomials and Daubechies' wavelets,* Technical Report 9301, Department of Mathematics, National Central University, 1993.

[12] G. Strang, *Wavelets and dilation equations: A brief introduction,* SIAM Review, 31 (1989), pp. 614–627.

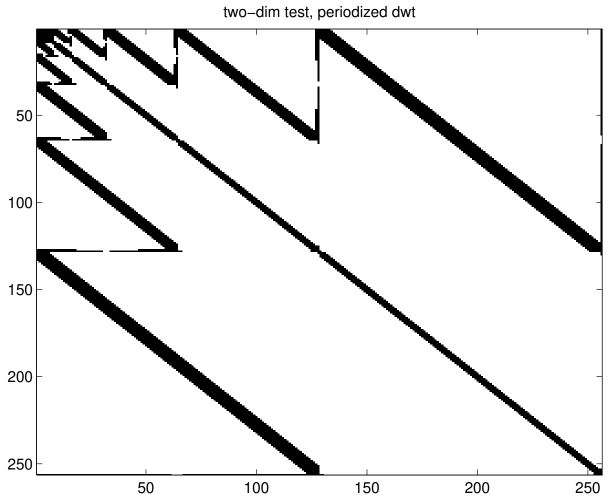

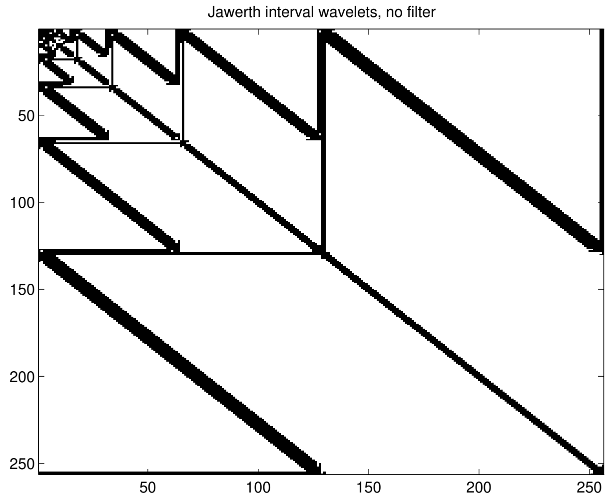

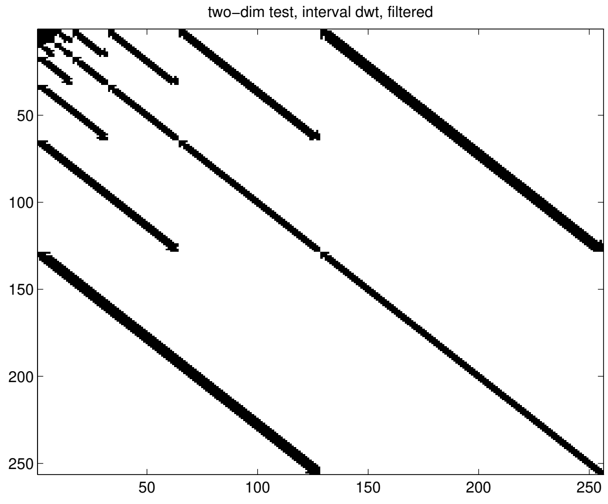

Figure 5. We choose the test two-dimensional data to be the 256×256 matrix $A = (a_{ij})$ where $a_{ij} = -1$ if $i = j$, and $a_{ij} = \frac{1}{\sqrt{|i-j|}}$ if $i \neq j$. Take periodized 2-d DWT of A, we show only the entries whose magnitude is larger than 0.1% of the maximum (top). Observe the black edges caused by the discontinuity introduced by the periodic extension. Similar to the one-dimensional case, the interval 2-d DWT has worse result (bottom left). The interval 2-d DWT with the filtering process completely eliminates the artificial large entries (bottom right). If we set the entries not shown on the graph by 0, then the compression rate has raised from 10.7 (top) to 14.3 (bottom right).